

Synthesis of bimetallic Zr(Ti)-naphthalendicarboxylate MOFs and their properties as Lewis Acid catalysis

Antonia M. Rasero-Almansa,^a Marta Iglesias,^a and Félix Sánchez^b

Supplementary Information

1. Materials and Methods

Reagents were purchased from commercial suppliers (Sigma-Aldrich, across, Scharlab); dried solvents were used. Reactions were performed under N₂ atmosphere when specified. The solids were characterized by the following techniques:

Elemental analyses were carried out on a Perkin-Elmer CHNS Analyzer 2400 and an Inductively Coupled Plasma Optical Emission Spectroscopy (ICP OES) Perkin Elmer 40 for metal determination.

TXRF were performed on Fluorescence Spectrometer Total reflection X-ray (TXRF) fixed geometry (S2 PICOFOX TXRF spectrometer). It consists of a detector SDD and acquisition electronics, an automatic exchanger up to 25 samples, a HV transformer integrated technology (50 kV, 600 μA, 50 W), a microsource anode X-ray of Mo and an optical single monochromator energy filter through superlattice Ni / C

Diffuse reflectance UV spectra of powdered samples diluted by with BaSO₄ were recorded on a UV-Vis Spectrophotometer Shimadzu, UV 1201 model.

Fluorescence was carried out on a Fluorescence Spectrophotometer Varian Cary Eclipse model. It consists of two slots of Czerny-Turner (excitation and emission) with double monochromator, a source of continuous xenon light emission between 190 nm and 900 nm. It has a range of fixed width slits and selectable filters.

FT-IR spectra were recorded between 4000 and 400 cm⁻¹ with a Bruker IFS 66V/S, using the KBr pellets technique (about 1 mg of sample and 300 mg of dry KBr were used in the preparation of pellets).

High resolution ¹³C **MAS or CP/MAS NMR**, spectra of powdered samples, were recorded at room temperature under magic angle spinning (MAS) on a Bruker AV-400-WB spectrometer equipped with an FT unit. The ¹³C cross-polarization (CP-MAS) spectra were acquired by using a contact time of 3.5 ms and recycle of 4 s. All spectra were recorded with a 4 mm ZrO probe and Kel-F plug and at sample spinning rate of 10 kHz.

X-Ray Diffraction (XRD) patterns were performed by a Bruker D8 diffractometer with a Sol-X energy dispersive detector, working at 40 kV and 30 mA and employing CuKα (λ = 1.5418 Å) filtered radiation. The diffractograms were registered with a step size of 0.02° and exposure time of 0.5 s per step and a 2θ range of 2-40°.

The textural properties were analyzed by N₂ adsorption/desorption experiments performed at -196 °C using a static volumetric apparatus, Micromeritics ASAP 2010 analyzer. The samples (150–200 mg) were outgassed, previous to the analysis, for 12 h at 80 °C, or till the outgassing pressure reached 5 mm Hg. For the analysis at low

relative pressure range, up to $P/P_0 = 0.05$, successive doses of nitrogen of $4 \text{ cm}^3 \text{ STP/g}$ were added, equilibrating for 1.5 h. Subsequently, the adsorption branch of the isotherm was obtained following a previously fixed 40-points P/P_0 table, and the desorption branch following a previously fixed 20-points P/P_0 table. The specific total surface area was calculated using the Brunauer–Emmett–Teller (BET) method¹, selecting the adsorption data respective to the P/P_0 between 0.05 and 0.2 (adjusting the C value from 50 to 150^2), considering a nitrogen molecule cross-section area value of 0.162 nm^2 .³ The external surface area and micropore volume was obtained by means of the t-plot according to De Boer's method⁴. The total pore volume (V_p) of the solids was estimated from the amount of nitrogen adsorbed at a relative pressure of 0.99, assuming that the density of the nitrogen condensed in the pores is equal to that of liquid nitrogen at $-196 \text{ }^\circ\text{C}$, i.e. 0.81 g/cm^3 .⁵ The pore size distributions of microporous and mesoporous regions have been performed by using, respectively, the Horvath–Kawazoe⁶ and the Barrett–Joyner–Halenda (BJH) methods⁷.

The **thermogravimetric and differential thermal analyses (TGA-DTA)** were performed using Seiko TG/DTA 320U equipment in the temperature range between 25 and $850 \text{ }^\circ\text{C}$ in air (100 mL min^{-1} flow) atmosphere and a heating rate of $10 \text{ }^\circ\text{C min}^{-1}$.

SEM analysis. Particle morphology and size were studied under a scanning electron microscope (SEM) (XL30, Philips) operating at 25 kV . One droplet ($15\text{--}20 \text{ }\mu\text{L}$) of the corresponding suspension was placed on a glass surface (14 mm diameter) and allowed to dry; after which, the sample was covered with gold using a sputter coating device (Polaron SC7640, Thermo VG Scientific).

X-ray photoelectron spectroscopy (XPS) Photoelectron spectra (XPS) were recorded using an Escalab 200R spectrometer provided with a hemispherical analyzer, operated in a constant pass energy mode and Mg $K\alpha$ X-ray radiation ($h \text{ } 1253.6 \text{ eV}$) operated at 10 mA and 12 kV .

Digestion and Analysis by $^1\text{H-NMR}$ and ES-MS.⁸ 6 mg of dried microcrystalline Zr-NDC or Zr-NDC- NH_2 were digested by sonication in $600 \text{ }\mu\text{L}$ of d_6 -DMSO and $30 \text{ }\mu\text{L}$ of HF_{aq} . After complete dissolution of the material, the solution was used to collect a ^1H NMR spectrum (recorded on an INNOVA Varian spectrometer (300 MHz)).

NH_3 -TPD was performed on a Micromeritics Autochem II 2920, the sample was pretreated at $150 \text{ }^\circ\text{C}$ for 1 h under He; After cooling to room temperature, the samples were saturated in an NH_3 stream and then purged with a helium flow at $100 \text{ }^\circ\text{C}$ for 1 h ; the TPD profile was determined by increasing temperature to $220 \text{ }^\circ\text{C}$ with a ramp of $5 \text{ }^\circ\text{C min}^{-1}$. The concentration of the desorbed ammonia was analyzed with a TCD detector.

2. Synthesis

Synthesis of $\text{Zr}_6\text{O}_4(\text{OH})_4(\text{R-COO}_2)_{4.8}(\text{RCOO}_2\text{-NH}_2)_{1.2}$ (R-COO₂ is BDC: 1,4-benzenedicarboxylic acid, BPDC: 4,4'-biphenyldicarboxylic acid and NDC: 2,6-naphthalenedicarboxylic acid).

Zirconium MOFs with mixed ligand were prepared and purified using a modified general synthesis⁹. ZrCl_4 (0.4 g , 1.7 mmol) in dimethylformamide (DMF) (75 mL) was dispersed by ultrasound at $50\text{--}60 \text{ }^\circ\text{C}$, acetic acid (2.85 mL , 850 mmol) was added. Dicarboxylic acid and amino-dicarboxylic acid 20% molar ratio in DMF solution (25 mL) was added to the clear solution and finally, water (0.125 mL , 0.007 mmol) was

added. The mixture was sonicated at 60 °C and kept in a bath at 120 °C under static conditions for 24 h. After 24 h, the solutions were cooled to room temperature and the precipitate was isolated by centrifugation and washed with DMF (10 mL) to remove the excess of unreacted dicarboxylic acid. Solid was stirred two times with tetrahydrofuran (THF) for 24 hours to thoroughly removing DMF; finally, the solid $Zr_6O_4(OH)_4(COO_2)_{4.8}(COO_2N)_{1.2}$ was dried under reduced pressure (100 °C, 3 h). (Yield: 85%).

Ti(IV)-UiO-MOFs and. $TiCl_4(THF)_2$ (38 mg, 0.1 mmol) was dissolved in DMF (6mL). UiO (50 mg, 0.3 mmol equiv of linker) was placed in a vial, and the solution of titanium was added. This mixture was incubated at 85 °C in a pre-heated oven for 5 days. After cooling was centrifuged and the solids washed with 3x10 mL of DMF, 10 mL of MeOH and 10 mL of THF. The final solids were dried at 100 °C under vacuum to yield: $Zr_{4.5}Ti_{1.5}O_4(OH)_4(BDC)_{4.8}(BDC-NH_2)_{1.2}$, $Zr_{4.5}Ti_{1.5}O_4(OH)_4(BPDC)_{4.8}(BPDC-NH_2)_{1.2}$; $Zr_{4.4}Ti_{1.6}O_4(OH)_4(NDC)_6$; $Zr_{4.3}Ti_{1.7}O_4(OH)_4(NDC)_{4.8}(NDC-NH_2)_{1.2}$.

3.-Characterization

Table S1. Elemental analysis

	%C (calc.)	%H (calc.)	%N (calc.)	Zr/Ti	
				EDX	TXRF
Zr-NDC	40.95 (43.75)	2.42 (2.65)	-		
Zr-NDC-NH ₂	39.28 (43.36)	2.53 (2.69)	0.87 (0.84)	-	-
Zr(Ti)-NDC	36.18 (45.34)	3.09 (2.75)	-	2.50	2.64
Zr(Ti)-NDC-NH ₂	32.28 (45.02)	2.09 (2.79)	1.23 (0.88)	2.47	2.50
UiO66(Ti)-NH ₂				2.75	3.10
UiO67(Ti)-NH ₂				2.82	3.00

Table S2. Textural properties.

	BET (m ² /g)	Pore size (nm)	V (cm ³ /g)
Zr-NDC	1068.7	1.48	0.27
Zr(Ti)-NDC	1062.6	2.07	0.53
Zr-NDC-NH ₂	1372.9	1.68	0.48
Zr(Ti)-NDC-NH ₂	1026.7	1.94	0.56

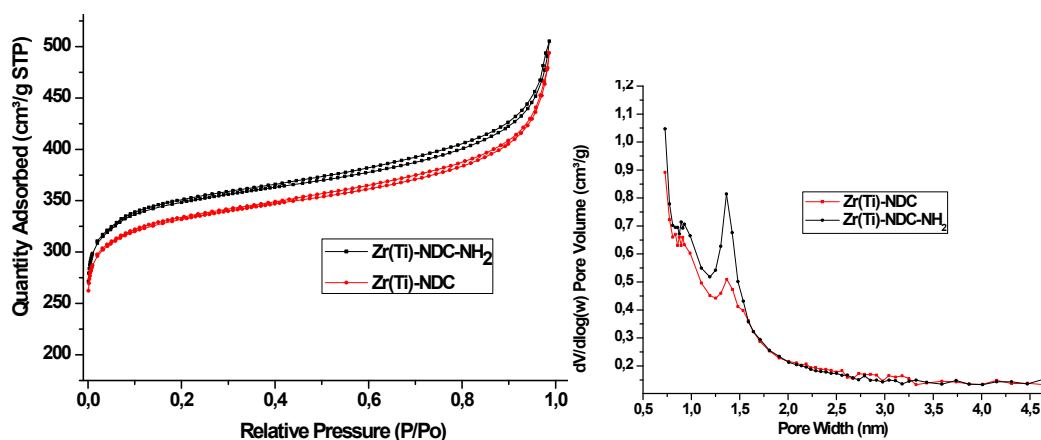


Figure S1. N₂ adsorption/desorption isotherms and pore distribution of Zr(Ti)-NDC materials.

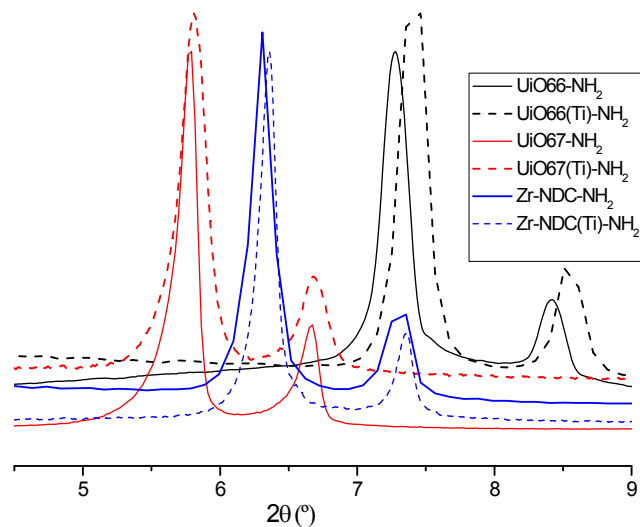


Figure S2. PXRD patterns of Zr-Linker-NH₂ and Zr(Ti)-Linker-NH₂.

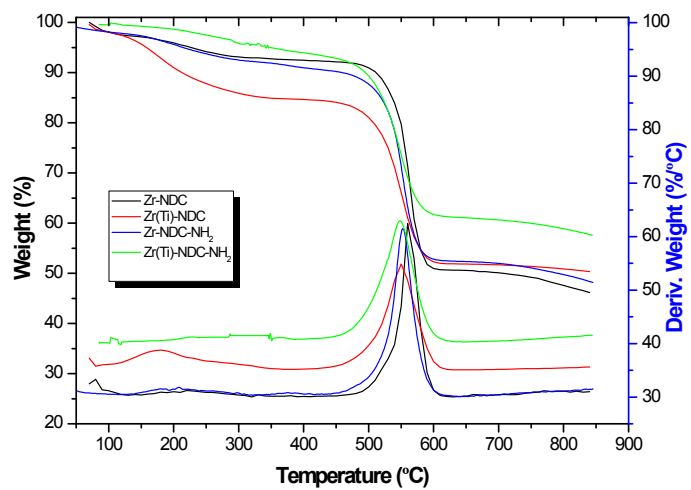


Figure S3. Thermograms of Zr-NDC series

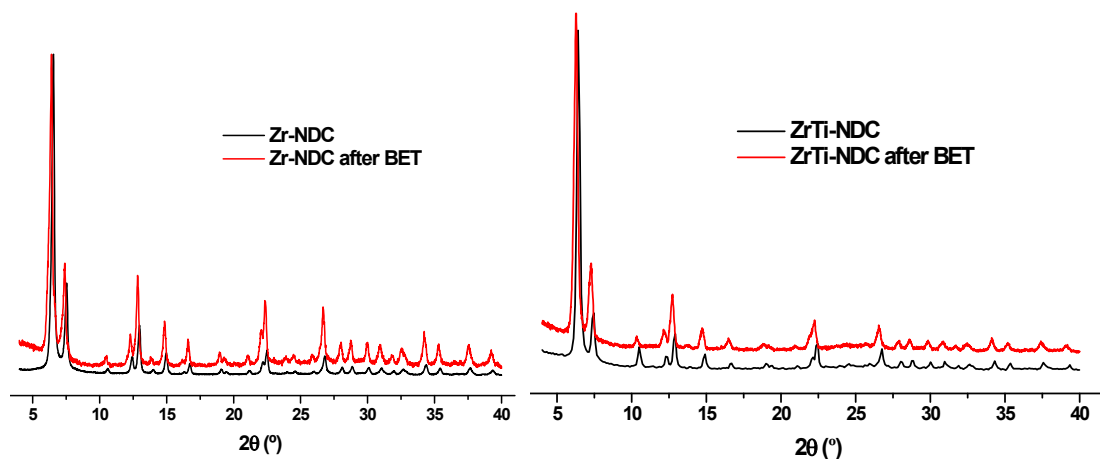


Figure S4a. PXRD patterns of Zr-NDC and Zr(Ti)-NDC fresh and after BET measurements.

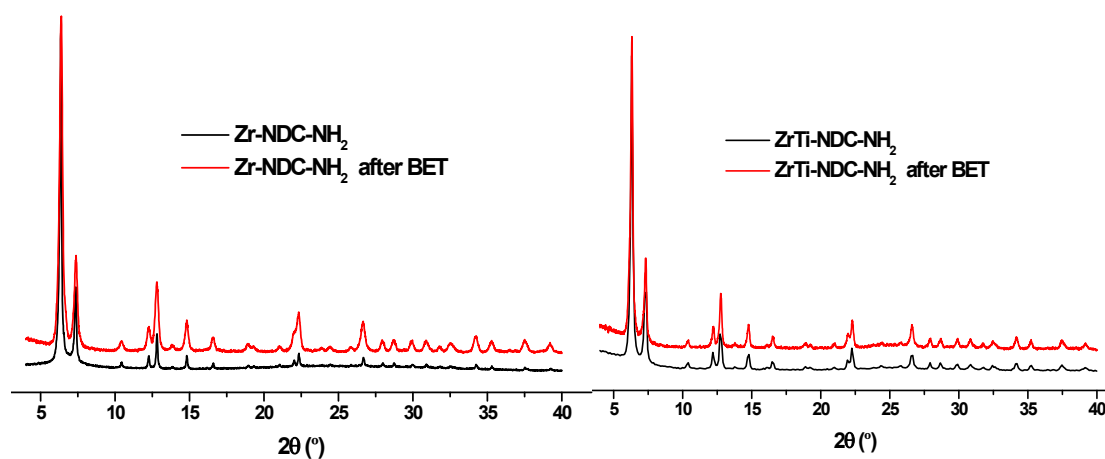


Figure S4b. PXRD patterns of Zr-NDC-NH₂ and Zr(Ti)-NDC-NH₂ fresh and after BET measurements.

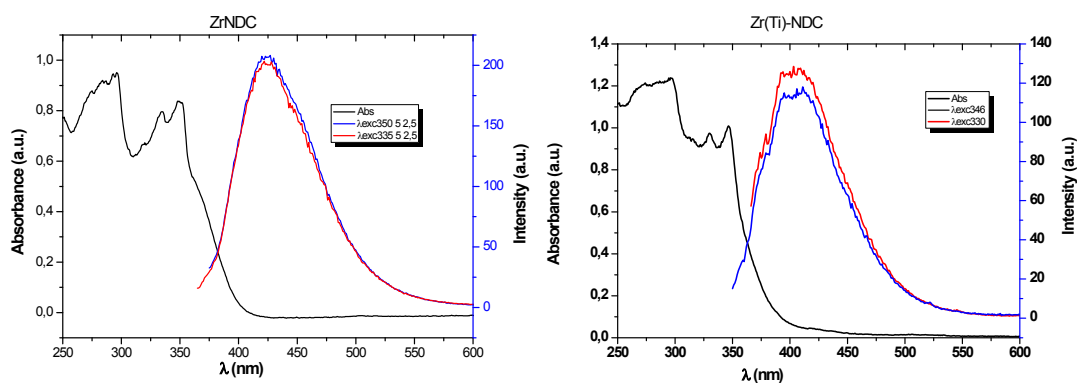


Figure S5a. Absorption-emission spectra of Zr-NDC, Zr(Ti)-NDC.

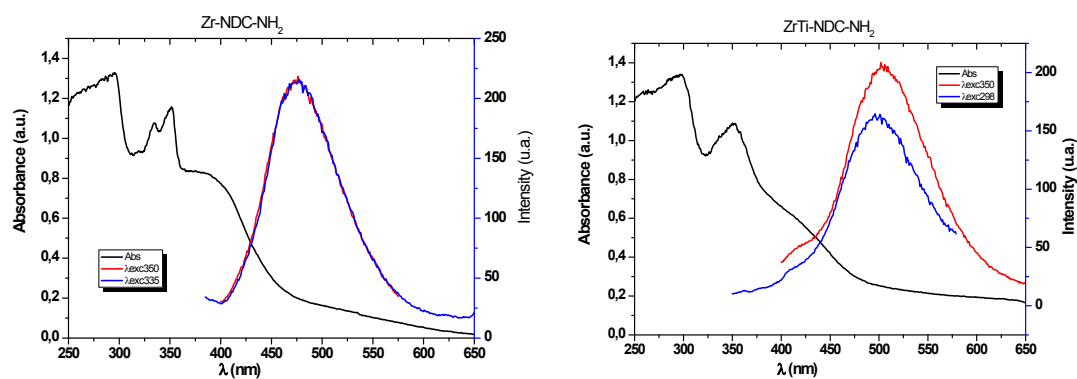


Figure S5b. Absorption-emission spectra of Zr-NDC-NH₂, Zr(Ti)-NDC-NH₂.

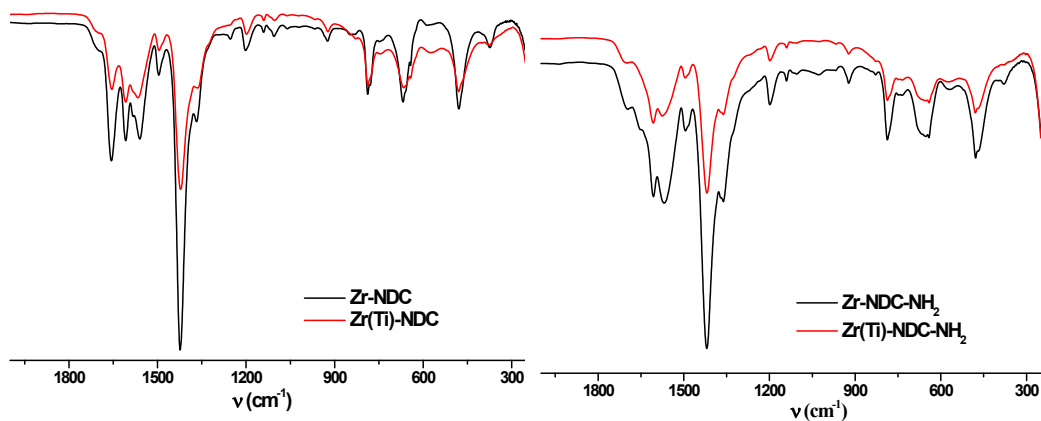
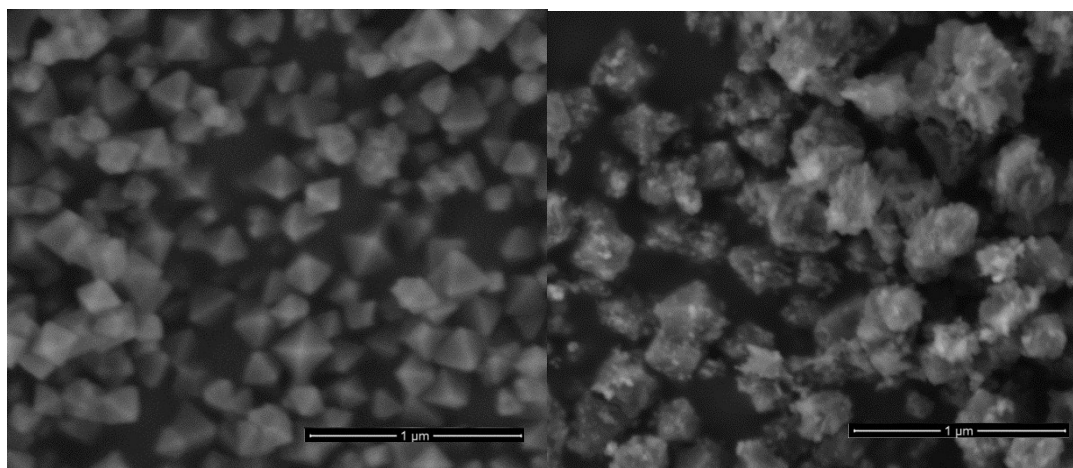
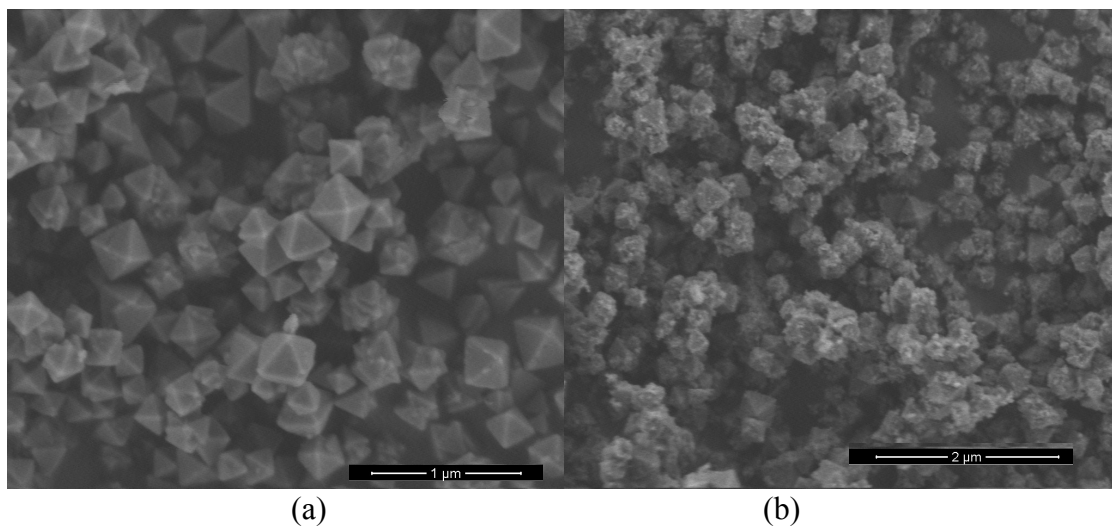


Figure S6. FTIR spectra: the anti-symmetric (1590-1550 cm⁻¹) and symmetric (1390-1370 cm⁻¹) stretches of the carboxylate groups are present in the spectra of all four compounds, respectively.



(a) (b)
Figure S7a. SEM images of (a) Zr-NDC, (b) Zr(Ti)-NDC.



(a) (b)
Figure S7b. SEM images of (a) Zr-NDC-NH₂, (b) Zr(Ti)-NDC-NH₂.

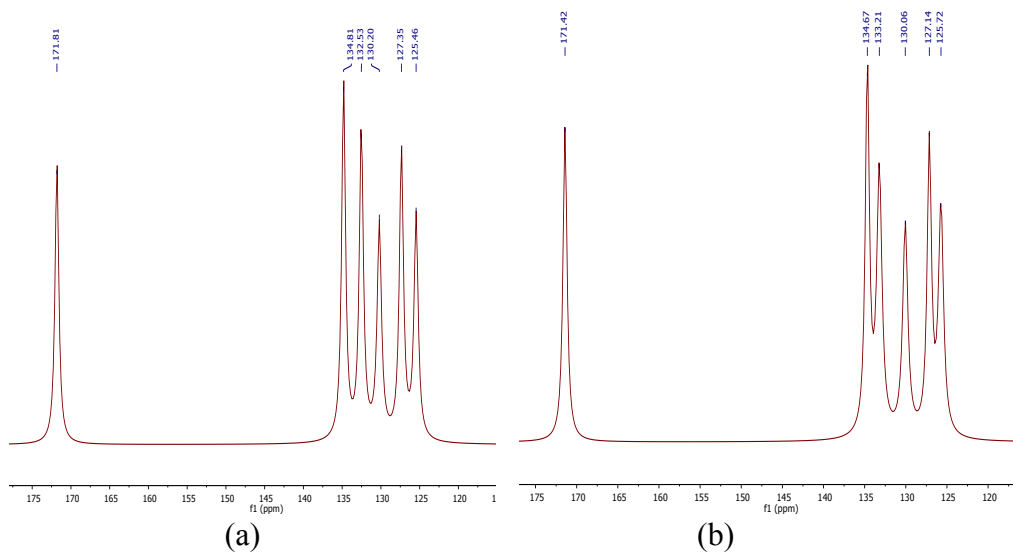


Figure S8a. ^{13}C -NMR spectrum of (a) Zr-NDC, (b) Zr(Ti)-NDC

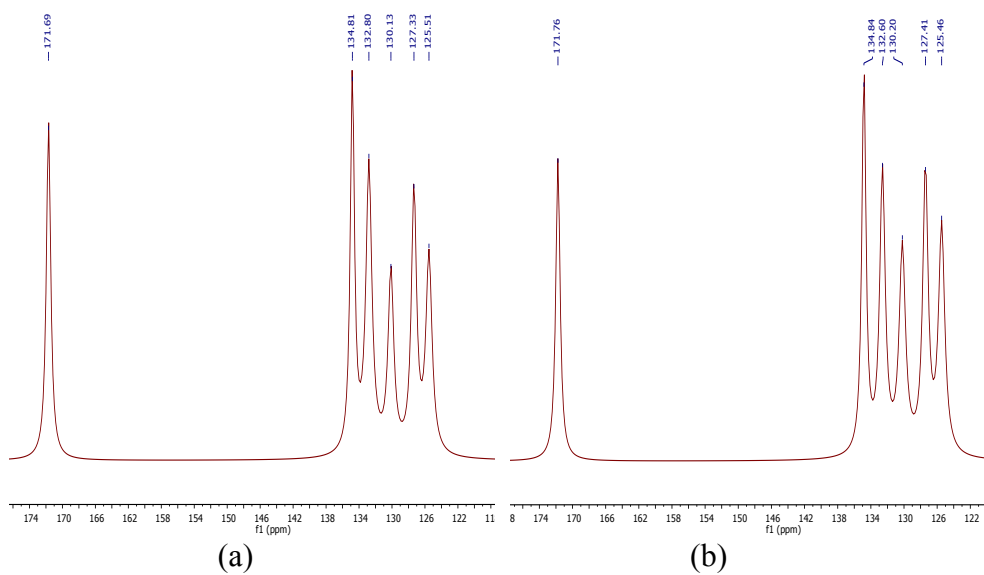
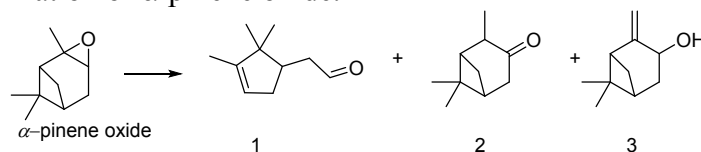


Figure S8b. ^{13}C -NMR spectrum of (a) Zr-NDC-NH₂, (b) Zr(Ti)-NDC-NH₂.

4.- Catalytic activity

Table S3. Isomerization of α -pinene oxide.



Catalyst	T (°C)	Solvent	% Conv. (h)	Sel. (%)		
				1	2	3
Zr-NDC	70	Toluene	37 (24)	47	22	31
Zr(Ti)-NDC	70	Toluene	65 (24)	51	21	28
Zr-NDC	70	-	61 (24)	48	30	22
Zr(Ti)-NDC	70	-	70 (24)	40	26	34
Zr-NDC	70	Dichloroethane	74 (24)	51	19	30
Zr(Ti)-NDC	70	Dichloroethane	88 (24)	55	20	25
Zr-NDC	100	Dichloroethane	64 (24)	45	20	35
Zr(Ti)-NDC	100	Dichloroethane	77 (24)	37	23	40
Zr-NDC	150	Dichloroethane	94 (6)	40	25	35
Zr(Ti)-NDC	150	Dichloroethane	97 (6)	29	16	55
Zr(Ti)-NDC	50	Dichloroethane	55(24)	40	29	31
Zr(Ti)-NDC	25	Dichloroethane	traces (24)	-	-	-

¹H-NMR for ether products

1-(sec-butoxymethyl)-4-methoxybenzene: oil, ¹H NMR (CDCl₃, 300 MHz) δ : 7.23 (d, J = 8.5 Hz, 2H, Ph), 6.86 (d, J = 8.5 Hz, 2H, Ph), 4.42 (s, 2H, OCH₂), 3.80 (s, 3H, OCH₃), 3.46 (m, 1H, OCH), 1.50 (m, 2H, CH₂), 1.20 (d, 3H, CH₃), 0.94 (t, J = 7.5 Hz, 3H, CH₃). ¹H NMR data are in good agreement with the literature data.¹⁰ GC-MS m/z = 194 (M⁺).

(sec-butoxymethyl)benzene. oil. ¹H NMR (CDCl₃, 300 MHz) δ : 7.75-8.0 (m, 3H), 7.42-7.6 (m, 2H), 4.55 (d, 1H), 4.50 (d, 1H), 3.52 (sextet, 1H), 1.60-1.75 (m, 1H), 1.45-1.60 (m, 1H), 1.20 (d, 3H), 1.0 (t, 3H) ppm; ¹H NMR data are in good agreement with the literature data.¹⁰ GC-MS m/z = 164 (M⁺).

4.- Characterization data of recovered catalysts

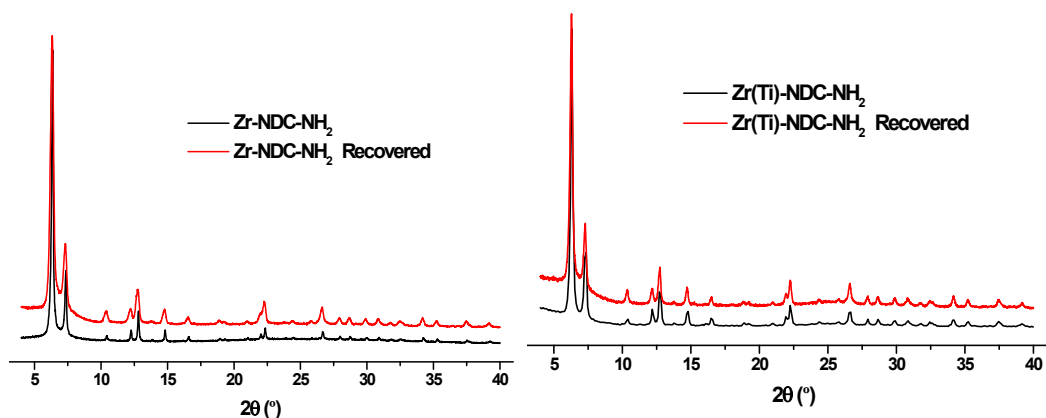


Figure S9a. PXRD of recovered Zr-NDC-NH₂ and Zr(Ti)-NDC-NH₂

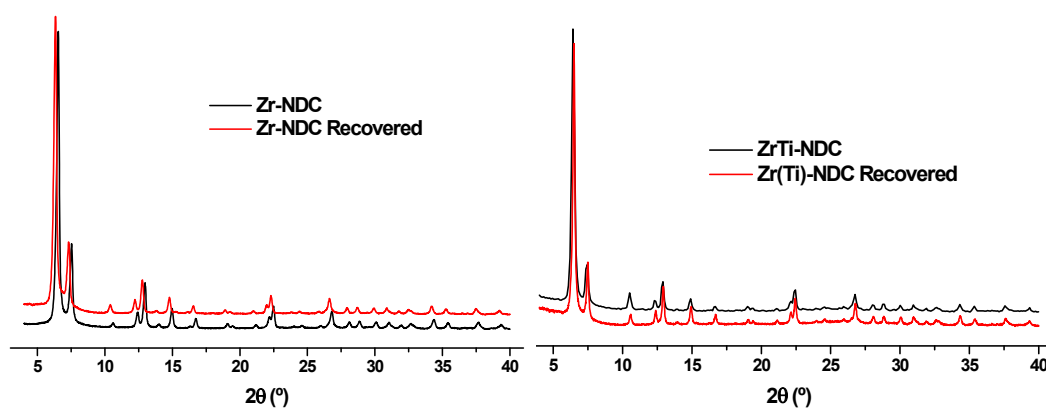


Figure S9b. PXRD of recovered Zr-NDC and Zr(Ti)-NDC.

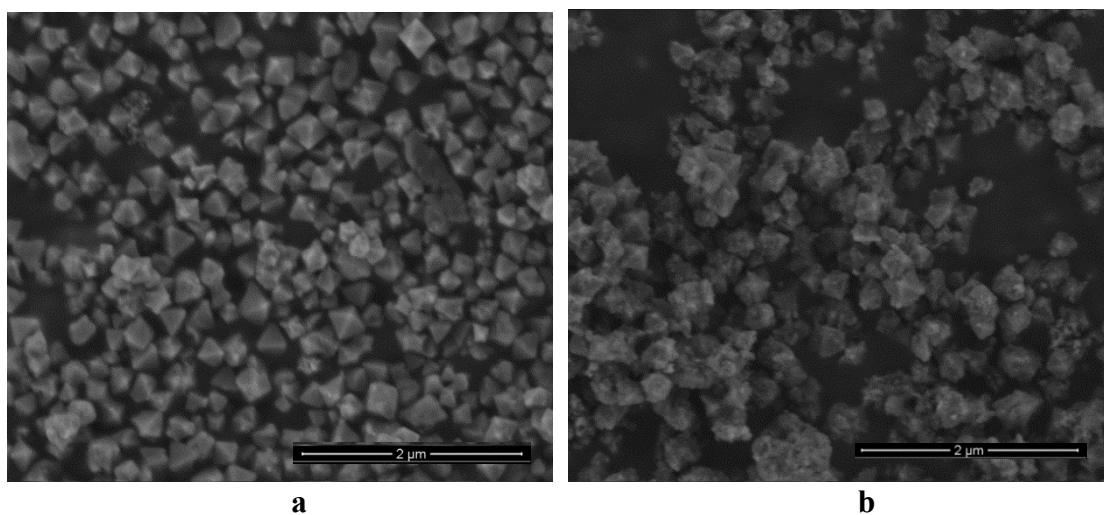


Figure S10a. SEM images of Zr-NDC (recovered) and S10b Zr(Ti)-NDC (recovered)

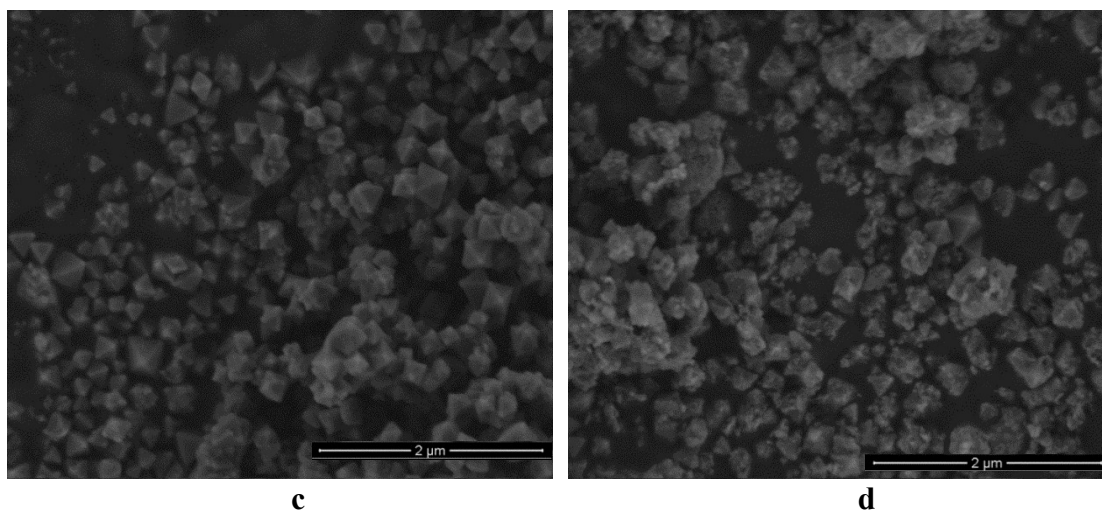


Figure S10c. SEM images of Zr-NDC-NH₂ (recovered), S10d Zr(Ti)-NDC-NH₂ (recovered).

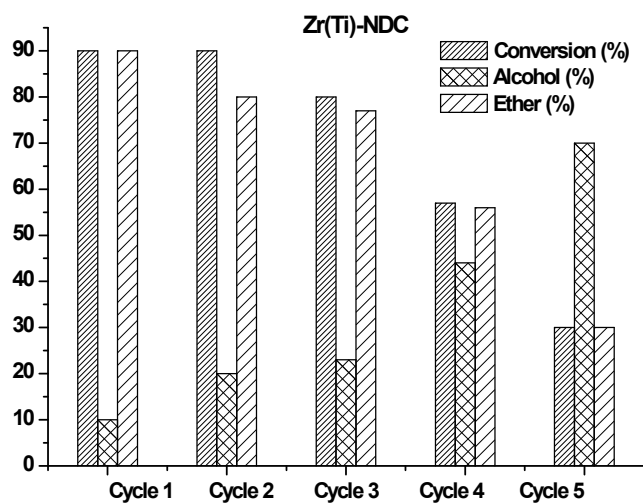


Figure S11. Recycling experiments for etherification reaction

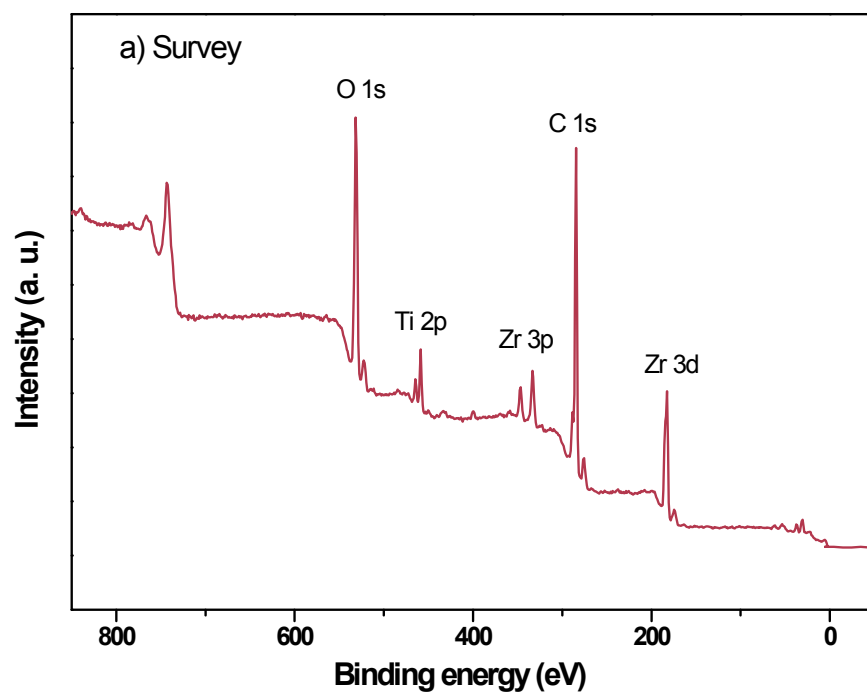


Figure S12. XPS spectra (survey scan) of Zr(Ti)NDC-NH₂

5.- Digestion and Analysis by $^1\text{H-NMR}$ and ES-MS

^1H NMR of digested Zr-MOF

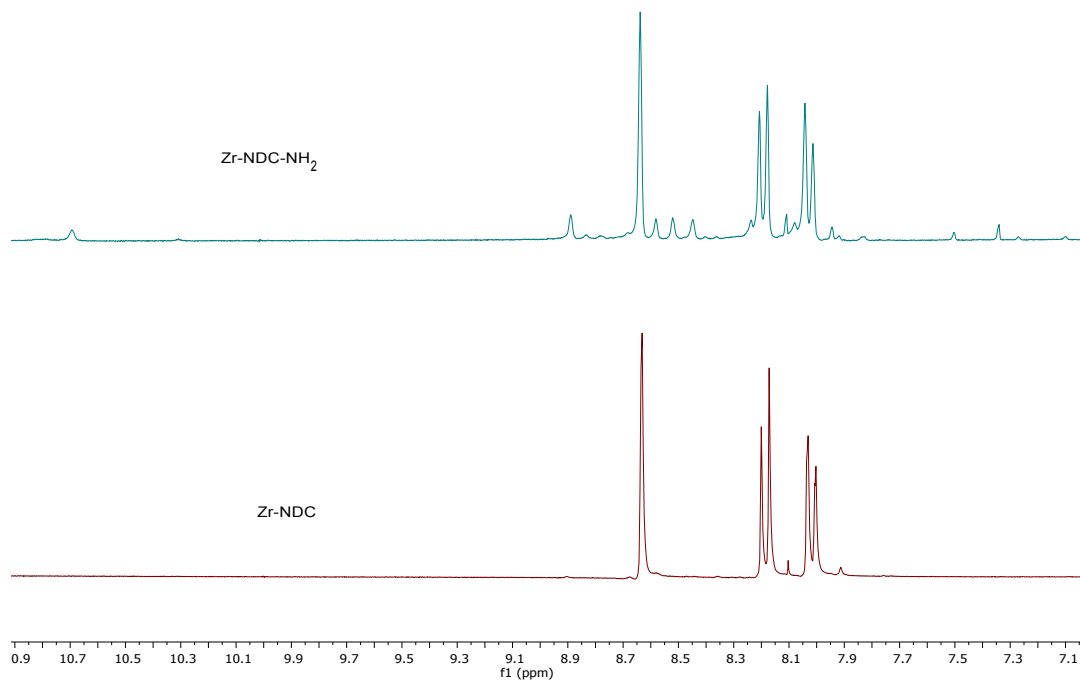


Figure S13. The ^1H NMR spectrum of a solution obtained by the digestion of Zr-NDC and Zr-NDC-NH₂ in DMSO-d₆/HF_{aq} mixture.

ES-MS spectra of digested Zr-MOF

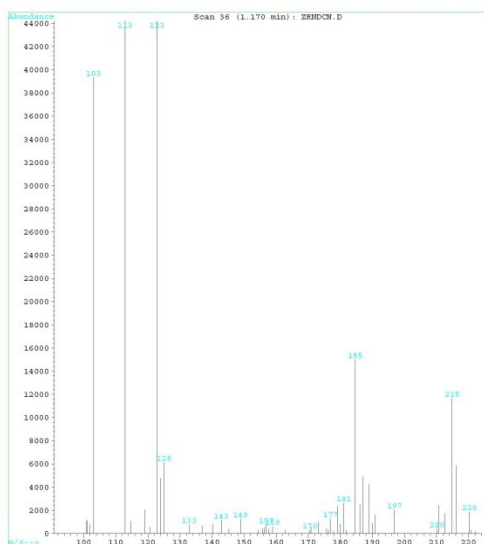


Figure S14a. Mass spectra showed a peak at m/z 215 corresponding to NDC linker. Last, HF cleaves also the Zr cluster itself, and the fluoro complex $[\text{ZrF}_5]^-$ is readily recognized in the mass spectra with a peak at m/z 185.

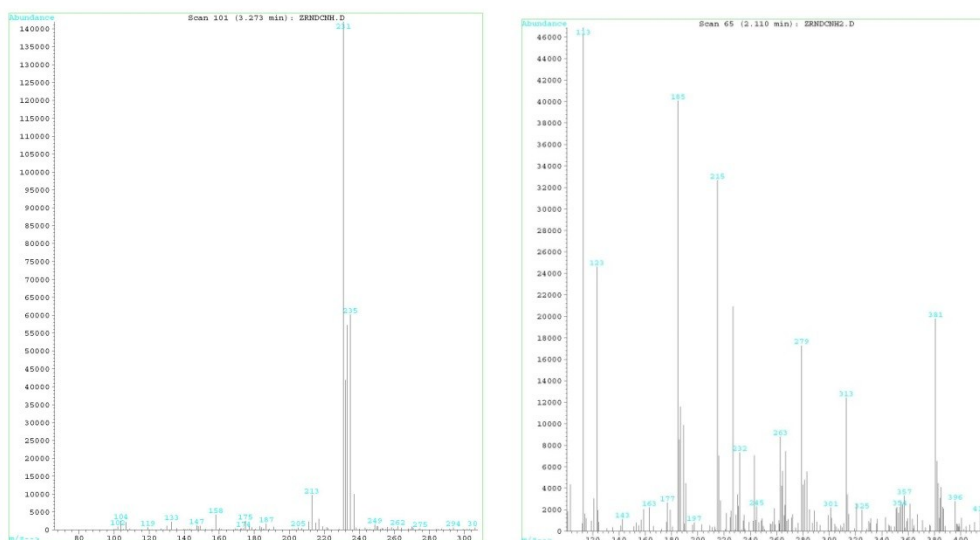


Figure S14b. Mass spectra showed peaks at m/z 215 (NDC linker) and 231 corresponding to NDC-NH₂ linker. Last, HF cleaves also the Zr cluster itself, and the fluoro complex [ZrF₅]⁻ is readily recognized in the mass spectra with a peak at m/z 185.

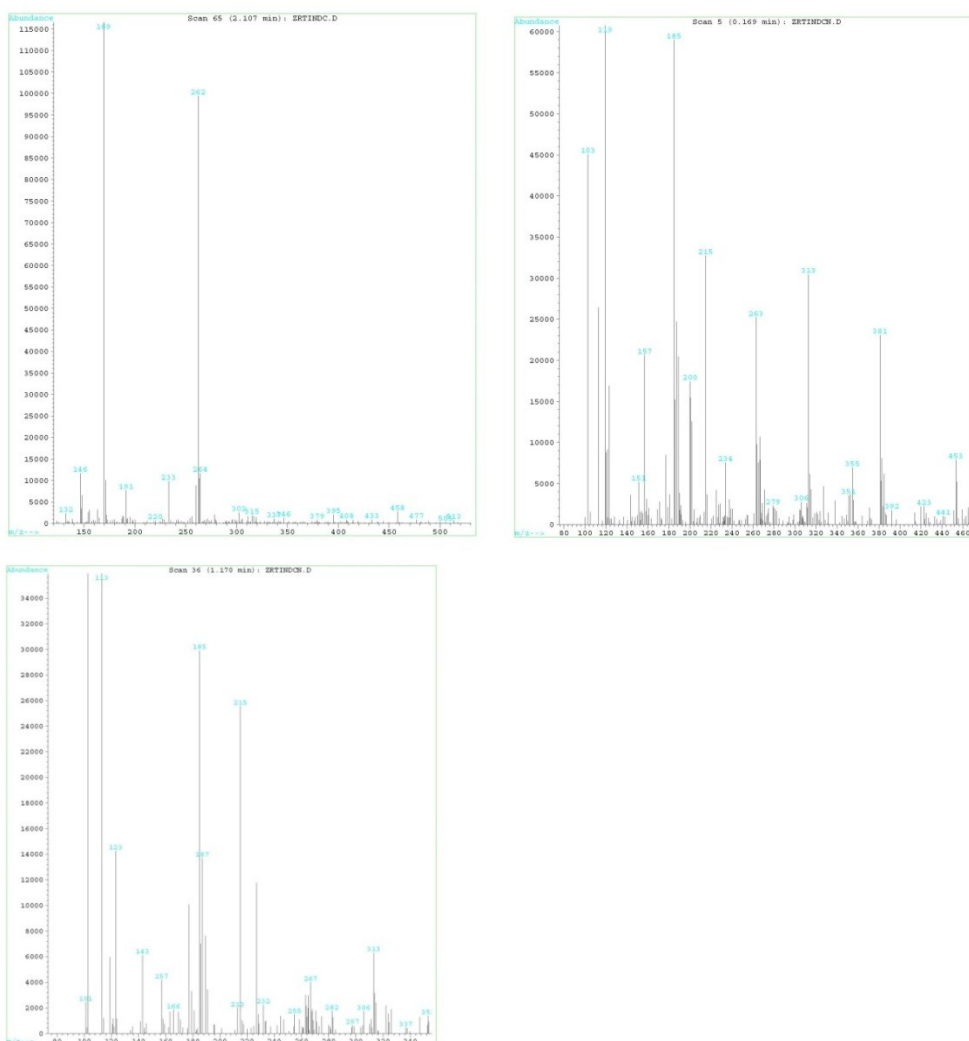


Figure S14c. Mass spectra showed peaks at m/z 215 (NDC linker), [ZrF₅]⁻ at m/z 185 and [TiF₅]⁻ at 143. A peak at m/z 263 corresponds to Ti-NDC fragment.

References

- ¹ S. Brunauer, P.H. Emmett, E. Teller, *J. Am. Chem. Soc.* 60 (1938) 309–319.
- ² K. S. W. Sing, *Colloids Surf. A* 187–188 (2001) 3–9.
- ³ F. Rouquerol, J. Rouquerol, K.S.W. Sing, *Adsorption by powders and porous solids, Principles, Methodology and Applications*, Academic Press, London, 1999.
- ⁴ B. C. Lippens, J. H. De Boer, *J. Catal.* 4 (1965) 319–323.
- ⁵ S. J. Gregg, K. S. W. Sing, *Adsorption, Surface Area and Porosity*, Academic Press, London, 1982
- ⁶ G. Horvath, K. Kawazoe, *J. Chem. Eng. Jpn.* 16 (1983) 470–475.
- ⁷ G. P. Barrett, L.G. Joyner, R. H. Halenda, *J. Am. Chem. Soc.* 73 (1951) 373–380.
- ⁸ S. J. Garibay, S. M. Cohen *Chem. Commun.*, 2010, 46, 7700-7702.
- ⁹ A. Schaate, P. Roy, A. Godt, J. Lippke, F. Waltz, M. Wiebcke, P. Behrens *Chem Eur J.* 17 (2011) 6643-6651
- ¹⁰ A. Corma, M. Renz; *Angew. Chem. Int. Ed. Eng.* 2007, 46, 298–300; N. Kalutharage, *Ch. S. Yi Org. Lett.* 2015, 17, 1778–1781